Spectral Enhancement in the Double Pulse Regime of Laser Proton Acceleration

K. Markey,[1,2,*] P. McKenna,[3] C. M. Brenner,[3,1] D. C. Carroll,[3] M. M. Günther,[4] K. Harres,[4] S. Kar,[2] K. Lancaster,[1] F. Nürnberg,[4] M. N. Quinn,[3] A. P. L. Robinson,[1] M. Roth,[4] M. Zepf,[2] and D. Neely[1]

[1]*Central Laser Facility, Rutherford Appleton Laboratory, Chilton, Didcot, Oxon OX11 0QX, United Kingdom*
[2]*School of Mathematics and Physics, Queen's University Belfast, Belfast BT7 1NN, United Kingdom*
[3]*SUPA, Department of Physics, University of Strathclyde, Glasgow G4 0NG, United Kingdom*
[4]*Institut für Kernphysik, Technische Universität Darmstadt, Schlossgartenstrasse 9, 64289 Darmstadt, Germany*

(Received 28 June 2010; published 5 November 2010)

The use of two separate ultraintense laser pulses in laser-proton acceleration was compared to the single pulse case employing the same total laser energy. A double pulse profile, with the temporal separation of the pulses varied between 0.75–2.5 ps, was shown to result in an increased maximum proton energy and an increase in conversion efficiency to fast protons by up to a factor of 3.3. Particle-in-cell simulations indicate the existence of a two stage acceleration process. The second phase, induced by the main pulse preferentially accelerates slower protons located deeper in the plasma, in contrast to conventional target normal sheath acceleration.

DOI: 10.1103/PhysRevLett.105.195008 PACS numbers: 52.38.Kd, 41.75.Jv, 52.38.Dx

The acceleration of protons and ions to MeV/amu energies using ultraintense laser pulses has become a widely studied area of intense laser plasma physics. Acceleration gradients of $\sim$ MV/μm are typically achieved over some tens of microns and result in beams of extremely low transverse and longitudinal emittance and extremely high peak particle flux (see [1] and references therein). A wide variety of applications has been suggested for such beams including nuclear physics, medical isotope production, ion beam therapy, isochoric heating of solids to warm dense matter states, and fast ignition ICF.

For p-polarized laser light at focused intensities of 10^{18}–10^{20} W/cm^2 the dominant laser-ion acceleration mechanism is target normal sheath acceleration (TNSA) [2]. TNSA has been extensively studied using the framework of self-similar plasma expansion theory [2,3]. However, analytical models usually employ simplified approximations of the density and temperature of the electrons and the effective acceleration time. As such, numerical simulations are needed to incorporate realistic absorption physics and temporally evolving particle distributions. Several theoretical and computational studies have investigated the effects of a temporally varying hot electron temperature [4–6] on the TNSA process. Robinson *et al.* simulated the effect of using two collinear intense pulses to generate two distinct hot electron temperatures during the acceleration [7]. It was found that control of the temporal variation of T_e, the hot electron temperature, on a subps time scale could lead to the formation of spectral modulations where at some energies, the proton numbers were greater than in the single pulse case.

Here we present the first experimental investigation of proton acceleration with a double pulse configuration similar to that proposed by Robinson *et al.*. The results indicate that a precisely controlled double pulse temporal intensity profile can lead to much higher conversion efficiency and increased peak proton energies. With the aid of 1D particle-in-cell (PIC) simulations the double pulse acceleration mechanism is shown to differ from the single pulse case in two ways. First, the laser absorption is increased due to the expansion of the target surface induced by the prepulse. Second, the prepulse preexpands the target rear surface. When the main pulse arrives, the strongest accelerating field is generated at a proton density modulation seeded by the heavy ions, rather than at the plasma-vacuum boundary as in the single pulse case.

The experiment was carried out using the Vulcan Petawatt laser system. Before power amplification the pulse was passed through a Mach-Zehnder style split-recombination system to introduce a controllable double pulse structure. The individual pulse length was 0.7 ps. A plasma mirror [8] was positioned at a suitable location along the focusing beam axis to ensure stable reflectivity during the reflection of both pulses but extremely low reflectivity prior to the arrival of the pulses to ensure a high contrast ratio. As the focusability degrades over the delay times used, the intensity ratio was preserved by avoiding tight focus. The focal diameter was 30 μm. The proton spectra were recorded with radiochromic film (RCF) stacks and Thomson parabola ion spectrometers. The RCF stack was centered along the rear target normal axis to capture the full beam flux. A slot in the stack enabled a small portion of the beam to propagate to the Thomson spectrometers, positioned along the rear target normal axis and 12° off the target normal. A photostimulable image plate was used to record the proton signal [9].

100 μm thick gold foils were used, somewhat thicker than those usually used in proton acceleration studies. While the conversion efficiency is lower, thicker foils greatly reduce any effects of hot electron recirculation,

which may also contribute to an enhancement in the acceleration [10], and also remove front surface accelerated protons from the spectra observed at the rear. Two ratios of setup pulse to main pulse energy or intensity were employed, 0.1:1 and 0.4:1. In each case the delay between the pulses was varied for successive shots.

The experimental results are presented in Fig. 1. For the 0.1:1 pulse ratio, the total energy on target was 130 J $\pm$ 10% and the main pulse intensity was 2.4×10^{19} W/cm^2 (increasing by 10% for zero delay). The RCF stack[Fig. 1(a)] recorded a significant increase in the proton flux at all energies for all double pulse shots at this ratio. The conversion efficiency to protons above 4 MeV peaked at 0.56% , at a delay of 1.5 ps. This was a factor of 3.3 greater than the conversion efficiency achieved with the single pulse. The Thomson spectra [Figs. 1(b) and 1(c)] all exhibit a low energy peak in the 2–3 MeV range, above which the protons exhibit a two temperature distribution, with a higher temperature towards the cutoff. Though the dip in signal below the low energy peak is not well characterized due to the lower energy limit of the detector, it does coincide with the maximum carbon or oxygen ion velocities, assuming the peak velocity of a species scales simply with the charge to mass ratio [11]. As with the RCF diagnostic, the proton signal over a broad range of energies was seen to be enhanced with the addition of a setup pulse. This enhancement was particularly strong at 12° off-axis [Fig. 1(c)]. The peak energy along the target normal axis was also increased from 15 MeV, for $\Delta t =$ 0 ps, to 20 MeV when $\Delta t = 1.5$ ps.

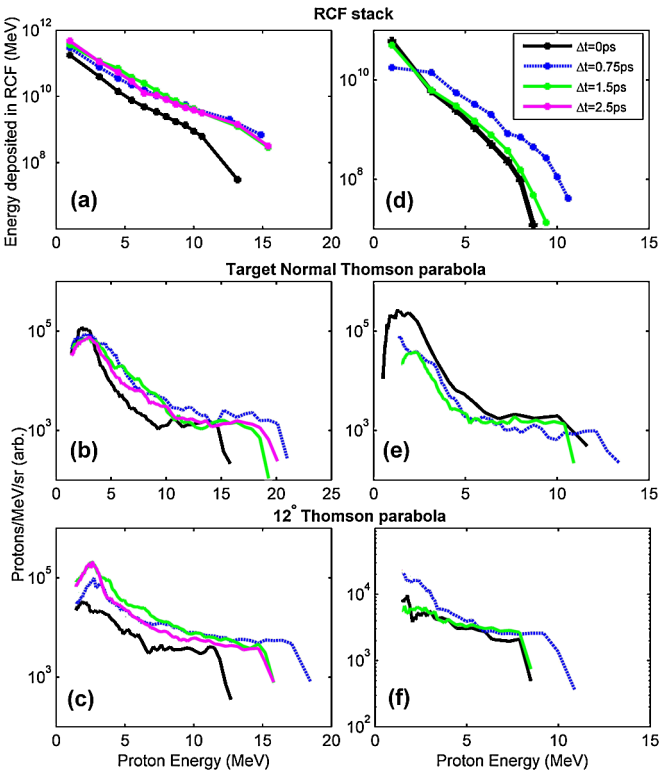

FIG. 1 (color online). Left: 0.1:1 ratio delay scan. (a) The proton energy deposited in the RCF stack was significantly greater for the double pulse shots, with conversion efficiency increased by a factor of ~3.3 when a prepulse was employed at a delay of 1.5 ps. Thomson spectra measured along (b) rear target normal axis and (c) at 12° to target normal also show marked increases in proton numbers and peak energies with the largest enhancement observed with the 12° spectrometer. Right: 0.4:1 ratio delay scan. (d) The 0.75 ps delay resulted in an increase in conversion efficiency by a factor of ~2.5, while (e) the target normal Thomson spectrometer indicated no enhancement. However the off-axis spectrometer (f) recorded a significant enhancement for the 0.75 ps delay. Note: Thomson spectra are plotted down to the lower detector limit.

For the 0.4:1 ratio delay scan, the total laser energy on target was 57 J $\pm$ 5%. The main pulse intensity on target was 8.3×10^{18} W/cm^2, (rising to 1.2×10^{19} W/cm^2 for zero delay), while the setup pulse intensity was 3.3×10^{18} W/cm^2. The lower laser energy used at this pulse ratio was due to the different beam splitters used in the delay control system. This reduced the typical conversion efficiencies by a factor of ~4. A pulse delay of 1.5 ps resulted in similar proton flux to the single pulse reference case [Fig. 1(d)]. However, the spectrum was significantly enhanced for an intermediate delay of 0.75 ps, with conversion efficiency increased by a factor of ~2.5 over the single pulse reference shot and the peak energy increased by ~20%. Along both Thomson spectrometer axes [Figs. 1(e) and 1(f)], the single pulse reference spectrum was similar in shape to that of the 0.1:1 ratio scan, with the peak energy reduced due to the lower laser energy or intensity available in this configuration. Correspondingly the low energy peak shifts to a slightly lower energy, in the vicinity of the detector cutoff. Along target normal, the single pulse shot actually resulted in higher signal than the double pulse spectra. The 0.75 ps delay yielded a higher peak energy but along target normal the proton signal was lower than in the single pulse case, in contrast to the angularly integrated RCF measurements. The 1.5 ps delay spectrum did not exhibit any significant increase in peak energy. However the 12° off-axis spectrometer detected a significant increase in proton numbers for the double pulse shots, at all energies. Clearly a comparison of the angularly integrated RCF measurements and the high resolution Thomson spectral data indicate that the increase in laser energy transfer to MeV protons shows a significant angular variation with a stronger enhancement at an angle to the beam propagation axis.

The enhancement in proton acceleration and its delay dependence are likely due to the competition of front and rear surface expansion. An increase in the plasma scale length at the front surface is known to increase laser absorption and proton acceleration [12], while expansion at the rear surface prior to the main pulse arrival has been shown to degrade the TNSA process [13,14].

1D particle- in-cell simulations were carried out to model the double pulse interaction dynamics and to account for the experimentally observed optimum pulse delay. Because of computational limitations it was not possible to simulate all the parameters at the full experimental values. The simulations do however represent a system where the laser target interaction, the ion-proton interaction and the final proton energies are comparable to the experiment. To accommodate realistic densities it was necessary to reduce the total number of particles and therefore a thinner target was used. The target was a 10 μm thick foil of heavy ions with charge $Z_i = +1$ and mass $m_i = 3m_p$ (m_p = proton mass) with a 20 nm layer of protons on each surface. The ion parameters were chosen to replicate the charge to mass ratio of C^{+4} while reducing the number of electrons needed. The initial ion and proton density was 8×10^{28} m^{-3}. The simulation box was 600 μm in length. The interaction was simulated up to 600 fs after t_0, the time at which the peak of the main laser pulse is incident on the target. The simulation runs differ only by the value of Δt, the pulse delay. For the first run Δt was 0 ps, i.e., a single Gaussian pulse of 300 fs FWHM duration. The peak intensity was 1.09×10^{20} W/cm^2. The other two runs employed the same laser energy divided between two pulses with delays of 0.75 and 1 ps. The prepulse to main pulse energy ratio was 0.4:1. The prepulse intensity was 3.14×10^{19} W/cm^2 and the main pulse intensity was 7.86×10^{19} W/cm^2. This intensity is higher than the experimental parameters. This is partly due to the shorter pulse duration employed. Also this intensity was chosen to match the experimental single pulse spectra. As the target surface is the same for both the single pulse and the prepulse, this ensures the expansion driven by the prepulse is also comparable to the experiment.

In the single pulse run a sharp plasma gradient is maintained during the entire interaction. The plasma expansion that would increase the scale length, and hence the absorption [15], is opposed by the ponderomotive force of the laser. The final energy spectrum is exponential with a small low energy modulation due to the heavy ions. The double pulse simulations show two features which contrast sharply with the single pulse case. First, during the time between the reflection of the prepulse and the arrival of the main pulse the plasma scale length at the front surface increases. This results in higher absorption of the main pulse into hot electrons. The second feature, only observed in the double pulse runs, is the presence of a rarefaction wave in the expanding proton layer at the rear surface (see Fig. 2). As the prepulse is sufficiently intense to heat electrons to hundreds of keV via the $J \times B$ mechanism [16], TNSA begins before the arrival of the main pulse. Note that experimentally the absorption and subsequent hot electron temperatures may be the cumulative effect of several multidimensional mechanisms [17], though the resultant electron temperatures generally scale with $I_L^{1/2}$. The rear surface plasma expansion induced by the prepulse, contains structure due to the presence of two ion species. A front is formed where the fastest ions cause protons in their vicinity to be accelerated beyond protons further from the front. This effect is visible in the proton phase space in Fig. 2(a). Protons accumulate in the region beyond the ion front. As such, the pure proton region contains a double layer structure of a slower dense region followed by a longer scale length exponential distribution of faster

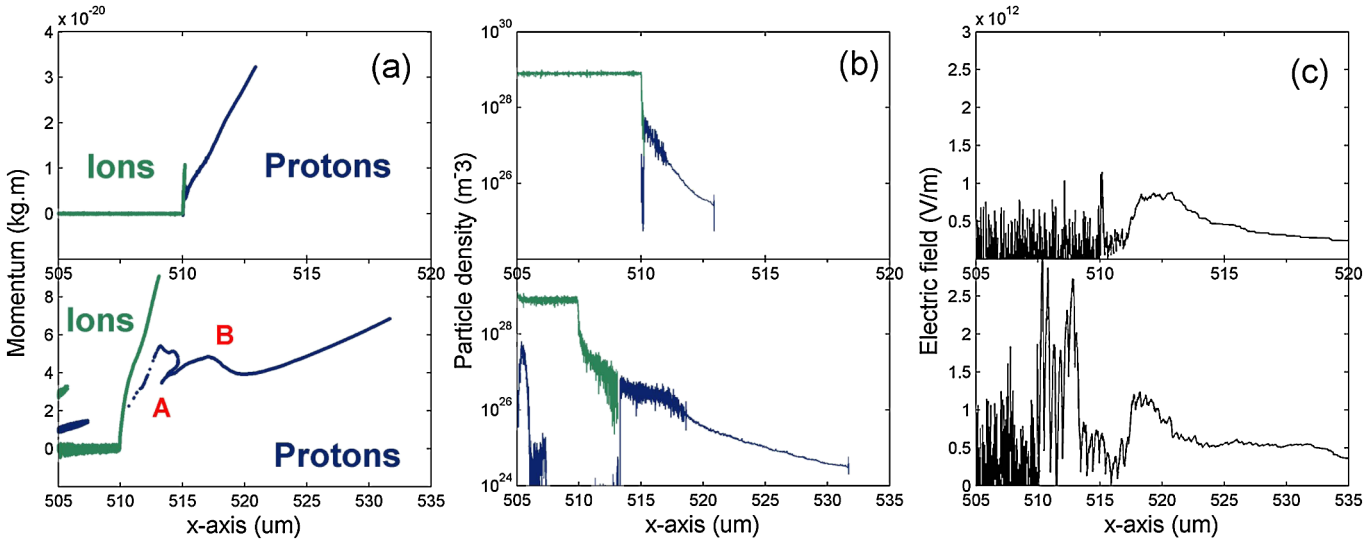

FIG. 2 (color online). Comparison of simulated interaction of a single pulse (top) at $t = t_0 + 100$ fs and a double pulse (bottom) with a 0.4:1 intensity ratio ($\Delta t = 0.75$ ps) at $t = t_0 + 50$ fs. (a) With a double pulse profile, proton repulsion from the ion front is much stronger and its effect on the proton phase space distribution is visible at the point labeled A. This drives a modulation in momentum space ahead of the ion front, labeled B. (b) A density modulation is formed in the expanding proton layer where (c) the local accelerating field is enhanced.

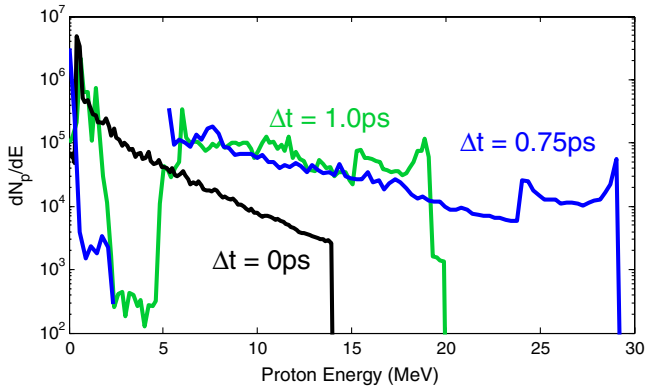

FIG. 3 (color online). Simulated proton spectra at $t = t_0 + 600$ fs. The highest peak proton energy and conversion efficiency were achieved with a pulse separation of 0.75 ps. In this case protons accelerated at the interface between the two proton layers achieve the highest energies. For the 1.0 ps delay the acceleration at both the proton-proton interface and the proton-vacuum interface is lower. Figures 1(d) and 1(f) show a very similar trend with pulse delay, albeit with less energy variation between the single and double pulse case.

protons. Such a profile can also be formed by the separation of the cold and hot electron populations as described by two temperature plasma expansion theory [18] and these processes may compliment one another. When the hot electron temperature is boosted by the arrival of the main pulse, the strongest accelerating field is generated at the interface of these two proton layers, rather than at the plasma-vacuum interface, as in the single pulse case. Protons at the edge of the slow dense layer surge forward and a rarefaction is observed to propagate as the denser proton layer expands faster than the less dense layer [see Fig. 2(b)]. The final proton spectra at $t = t_0 + 600$ fs are shown in Fig. 3. Rear surface expansion increases with longer pulse delay while the laser absorption begins to saturate. For rear surface expansion velocities comparable to the experiment, the simulations display an optimum pulse delay around 0.75 ps, where both the maximum proton energy and efficiency are reached. The double pulse runs result in energies substantially higher than the experimental results. This is believed to be due to the steplike surface profile assumed in the simulations. This leads to very low absorption of the first pulse, requiring a higher intensity to achieve the same peak energies as the experiment. The scale length increases so that by the time of the main pulse arrival the absorption is increased by approximately an order of magnitude, resulting in much higher proton energies. By assuming a small finite front surface gradient the relative absorption of the two pulses could be more accurately simulated, allowing lower intensities to be used to generate the experimental expansion velocities.

The PIC simulations support the experimental findings of increased proton energy and conversion efficiency over a finite range of pulse delays. However, several features of the experiment cannot be modeled by the 1D simulation. Multiple heavy ion charge states in the experiment may complicate the direct comparison with simulation. The radial variation in the spectral enhancement may be due to a variation in the optimal pulse delay with viewing angle due to the radial variation of rear surface expansion. These higher dimensional effects do not alter the main findings of the experiment and simulations.

These results indicate that proton beam generation via a double pulse configuration offers significantly greater scope for source optimization, particularly in areas where preheat by the fastest particles is detrimental to the application. Increases in conversion efficiency by a factor of 3.3 have been experimentally demonstrated for constant laser energy and target parameters. The highest efficiencies yet reported have been achieved with somewhat higher laser energy and much thinner foils [19–21]. As these studies were carried out with single pulses it is important to investigate the effectiveness of the double pulse technique for similar laser and target parameters. A tailored laser intensity profile would be an important feature of an optimized laser-proton source dedicated to applications such as ICF and isotope production.

We acknowledge the expert assistance of the Vulcan operations team. This work was supported by the UK Engineering and Physical Sciences Research Council (grant number EP/E035728/1 and EP/E048668/1) and the Bundesministerium für Bildung und Forschung, BMBF, support code 06 DA 9044I. M. Z. acknowledges support from the Royal Society.

*keith.markey@stfc.ac.uk

[1] M. Borghesi *et al.*, Fusion Sci. Technol. **49**, 412 (2006).
[2] S. C. Wilks *et al.*, Phys. Plasmas **8**, 542 (2001).
[3] P. Mora, Phys. Rev. Lett. **90**, 185002 (2003).
[4] P. Mora, Phys. Rev. E **72**, 056401 (2005).
[5] M. Passoni *et al.*, Phys. Rev. E **69**, 026411 (2004).
[6] V. T. Tikhonchuk *et al.*, Plasma Phys. Controlled Fusion **47**, B869 (2005).
[7] A. P. L. Robinson *et al.*, Plasma Phys. Controlled Fusion **49**, 373 (2007).
[8] B. Dromey *et al.*, Rev. Sci. Instrum. **75**, 645 (2004).
[9] A. Mančić *et al.*, Rev. Sci. Instrum. **79**, 073301 (2008).
[10] A. J. Mackinnon *et al.*, Rev. Sci. Instrum. **75**, 3531 (2004).
[11] M. Allen *et al.*, Phys. Rev. Lett. **93**, 265004 (2004).
[12] P. McKenna *et al.*, Laser Part. Beams **26**, 591 (2008).
[13] M. Borghesi *et al.*, Phys. Rev. Lett. **92**, 055003 (2004).
[14] J. Fuchs *et al.*, Phys. Rev. Lett. **99**, 015002 (2007).
[15] R. Nuter *et al.*, J. Appl. Phys. **104**, 103307 (2008).
[16] S. C. Wilks *et al.*, Phys. Rev. Lett. **69**, 1383 (1992).
[17] S. C. Wilks and W. L. Kruer, IEEE J. Quantum Electron. **33**, 1954 (1997).
[18] J. E. Crow *et al.*, J. Plasma Phys. **14**, 65 (1975).
[19] R. A. Snavely *et al.*, Phys. Rev. Lett. **85**, 2945 (2000).
[20] J. Fuchs *et al.*, Nature Phys. **2**, 48 (2006).
[21] L. Robson *et al.*, Nature Phys. **3**, 58 (2007).